SUGAR: Efficient Subgraph-level Training via Resource-aware Graph Partitioning

Zihui Xue, Yuedong Yang, Mengtian Yang, and Radu Marculescu

The University of Texas at Austin

arXiv:2202.00075v3 [cs.LG] 16 Feb 2022

***Abstract*—Graph Neural Networks (GNNs) have demonstrated a great potential in a variety of graph-based applications, such as recommender systems, drug discovery, and object recognition. Nevertheless, resource-efficient GNN learning is a rarely explored topic despite its many benefits for edge computing and Internet of Things (IoT) applications. To improve this state of affairs, this work proposes efficient subgraph-level training via resource-aware graph partitioning (SUGAR). SUGAR first partitions the initial graph into a set of disjoint subgraphs and then performs local training at the subgraph-level. We provide a theoretical analysis and conduct extensive experiments on five graph benchmarks to verify its efficacy in practice. Our results show that SUGAR can achieve up to 33× runtime speedup and 3.8× memory reduction on large-scale graphs. We believe SUGAR opens a new research direction towards developing GNN methods that are resource-efficient, hence suitable for IoT deployment.**

I. Introduction

Graphs are non-Euclidean data structures that can model complex relationships among a set of interacting objects, for instance, social networks, knowledge graphs, or biological networks. Given the huge success of deep neural networks for Euclidean data (*e.g.*, images, text and audio), there is an increasing interest in developing deep learning approaches for graphs too. Graph Neural Networks (GNNs) generalize the convolution operation to the non-Euclidean domain [26]; they demonstrate a great potential for various graph-based applications, such as node classification [14], link prediction [28] and recommender systems [6].

The rapid development of smart devices and IoT applications has spawned a great interest in many edge AI applications. Training models locally becomes a growing trend as this can help avoid data transmission to the cloud, reduce communication latency, and better preserve privacy [12]. For instance, in a graph-based recommender system, user data can be quite sensitive and hence it's better to store it locally [24]. This brings about the need for *resource-efficient graph learning*.

While there is much discussion about locally training Convolutional Neural Networks (CNNs) [1], efficient on-device training for GNNs is rarely explored. Different from CNNs, where popular models such as ResNet [10] are deep and have a large parameter space, mainstream GNN models are shallow and more lightweight. However, the major bottleneck of GNN training comes from the nodes dependencies in the input graph. Consequently, graph convolution suffers from a high computational cost, as the representation of a node in the current layer needs to be computed recursively by the representations of all neighbors in its previous layer. Moreover, storing the intermediate features for all nodes requires much memory space, especially when the graph size grows. For instance, for the *ogbn-products* graph in our experiments (Table I), full-batch training requires a GPU with 33GB of memory [11]. Thus scaling GNN training to large-scale graphs remains a big challenge. The problem is more severe for a resource-constrained scenario like IoT, where GNN training is heavily constrained by the computation, memory, and communication costs.

Various approaches have been proposed to alleviate the computation and memory burden of GNNs. For instance, sampling-based approaches aim at reducing the neighborhood size via layer sampling [2], [3], [9], clustering based sampling [5] and graph sampling [27] techniques; these prior works approach this problem purely from an algorithmic angle. A few recent works [23], [30] investigate the topic of distributed multi-GPU training of GNNs and achieve good parallel efficiency and memory scalability while using large GPU clusters.

A common limitation of all these approaches is that they *do not* take the real hardware constraints into consideration. For mobile devices with limited memory budgets, the input graph can be too large to fit entirely in the main memory. In addition, the communication overhead among real IoT devices is significantly larger than when using GPU clusters, rendering distributed training approaches not readily applicable to such scenarios. This calls for a new approach for *resource-efficient GNN learning*, which is precisely the focus of our paper.

In this work, we propose a novel approach that trains GNNs efficiently with multiple devices in a resource-limited scenario. To this end, we (1) design a graph partitioning method that accounts for resource constraints and graph topology; (2) train a set of local GNNs at the *subgraph-level* for computation, memory and communication savings. Our contributions are as follows:

- We formulate the problem of training GNNs with multiple resource-constrained devices. Although our formulation targets various mobile and edge devices (*e.g.*, mobile phones, Raspberry Pi), it is also applicable to powerful machines equipped with GPUs.
- We propose SUGAR, a GNN training framework that aims at improving training scalability. We provide complexity analysis, error bound and convergence analysis of the proposed estimator.

- We show that SUGAR achieves the best runtime and memory usage (with similar accuracy) when compared against state-of-the-art GNN approaches on five large-scale datasets and across multiple hardware platforms, ranging from edge devices (*i.e.*, Raspberry Pi, Jetson Nano) to a desktop equipped with powerful GPUs.
- We illustrate the flexibility of SUGAR by integrating it with both full-batch and mini-batch algorithms such as GraphSAGE [9] and GraphSAINT [27]. Experimental results demonstrate that SUGAR can achieve up to 33× runtime speedup on *ogbn-arxiv* and 3.8× memory reduction on *Reddit*. On the *ogbn-products* graph with over 2 million nodes and 61 million edges, SUGAR achieves 1.62× speedup over GraphSAGE and 1.83× memory reduction over GraphSAINT with a better test accuracy ($\sim$0.7%).

The remainder of the paper is organized as follows. In Section 2, we discuss prior work. In Section 3, we formulate the problem and describe our proposed training framework SUGAR. Experimental results are presented in Section 4. Finally, Section 5 concludes the paper.

II. Related Work

The relevant prior work comes from three directions as discussed next.

A. Graph Neural Networks

Modern GNNs adopt a neighborhood aggregation scheme to learn representations for individual nodes or the entire graph. Graph Convolution Network (GCN) [14] is a pioneering work that generalizes the use of regular convolutions to graphs. GraphSAGE [9] provides an inductive graph representation learning framework. To improve the representation ability of GNNs, Graph Attention Networks (GAT) [21] introduce self-attention to the graph convolution operation. Apart from pursuing higher accuracy, a few GNN architecture improvements [7], [25] have been made towards higher training efficiency.

B. GNN training algorithms

Current GNN training algorithms can be categorized into full-batch training and mini-batch training.

Full-batch training was first proposed for GCNs [14]; the gradient is calculated based on the global graph and updated once per epoch. Despite being fast, full-batch gradient descent is generally infeasible for large-scale graphs due to excessively large memory requirements and slow convergence.

Mini-batch training was first proposed in GraphSAGE [9]; the gradient update is based on a proportion of nodes in the graph and updated a few times during each training epoch. Mini-batch training leads to memory efficiency at the cost of increased computation. Since the neighborhood aggregation scheme involves recursive calculation of a node's neighbors layer by layer, time complexity becomes exponential with respect to the number of GNN layers; this is known as the *neighborhood expansion problem*.

Following the idea of neighbor sampling, FastGCN [3] further proposes the importance node sampling to reduce variance. The work of [2] proposes a control variate based algorithm that allows a smaller neighbor sample size.

A few recent works propose alternative ways to construct mini-batches instead of layer-wise sampling. For instance, ClusterGCN [5] first partitions the training graph into clusters and then randomly groups clusters together as a batch. GraphSAINT [27] builds mini-batches by sampling the training graph and ensures a fixed number of nodes in all layers.

C. Graph Sparsification

Recent works have also investigated graph sparsification (*i.e.*, pruning edges of the training graph) for GNN learning. In many real-world applications, graphs exhibit complex topology patterns. Some edges may be erroneous or task-irrelevant, and thus aggregating this information weakens the generalizability of GNNs [18]. As shown by [20] and [29], edges of the input graph may be pruned without loss of accuracy.

Two recent works introduce computation efficiency into the problem. More precisely, SGCN [17] proposes a neural network that prunes edges of the input graph; they show that using sparsified graphs as the new input for GNNs brings computational benefits. UGS [4] presents a graph lottery ticket type of approach; they sparsify the input graph, as well as model weights during training to save inference computation.

III. Our Proposed Method

A. Problem Formulation

Given a graph $\mathcal{G} = (\mathcal{V}, \mathcal{E})$, where $\mathcal{V}$ is the node set and $\mathcal{E}$ represents the set of edges. Let $N = |\mathcal{V}|$ denote the number of nodes and $A \in R^{N \times N}$ be the adjacency matrix of $\mathcal{G}$. Every node i is characterized by a F-dimensional feature vector $x_i \in R^F$. We use $X \in R^{N \times F}$ to represent the feature matrix of all nodes in $\mathcal{G}$.

Consider a node-level prediction problem with the following objective:

$$\min_W \mathcal{L} = \frac{1}{N} \sum_{i=1}^{N} f(y_i, z_i) \qquad z_i = g(x_i; W) \tag{1}$$

where f is the objective function (*e.g.*, cross entropy for node classification), y_i and z_i denotes the true label and prediction of node i, respectively. $g(\cdot)$ denotes a graph neural network parameterized by W that generates node-level predictions.

Suppose there are K devices available for training, and let $\mathcal{B}^k_{MEM}$ denote the memory budget of device k. Motivated by the notorious inefficiency that centralized graph learning suffers from, we aim at *distributing the training process* to improve the training scalability. The key is to assign N nodes of graph $\mathcal{G}$ to K devices, and then do local training on *each* device. We formulate it as two subproblems below.

First, we define a graph partitioning strategy $\mathcal{P} : \mathcal{V} \rightarrow (\mathcal{V}_1, \mathcal{V}_2, \cdots, \mathcal{V}_K)$ that divides the node set $\mathcal{V}$ into K subsets such that:

$$\cup_k \mathcal{V}_k = \mathcal{V}, \quad H(\mathcal{SG}_k) < \mathcal{B}^k_{MEM}, \quad \forall k \in [K] \tag{2}$$

where $[K] = \{1, ..., K\}$, $\mathcal{SG}_k$ denotes the subgraph induced by node set $\mathcal{V}_i$, H is a static function that maps a given subgraph $\mathcal{SG}_i$ to the device memory requirements for training. For maximum generality, here we do not require $\mathcal{V}_i \cap \mathcal{V}_j = \varnothing$. In other words, a node i can be assigned to more than one hardware device, and let $\mathcal{P}_i$ denote the set of hardware devices where node i is assigned to.

Next, we adopt subgraph-level training, *i.e.*, for device k, we maintain a local GNN model, denoted by $W^{\langle k \rangle}$ that takes the subgraph $\mathcal{SG}_k$ as its input graph. Let $W = \frac{1}{K}\sum_{k=1}^{K} W^{\langle k \rangle}$, thus the objective can be reformulated as:

$$\begin{aligned} \min_{W} \mathcal{L} &= \frac{1}{N}\sum_{i=1}^{N} f(y_i, z_i) \\ z_i &= \frac{1}{|\mathcal{P}_i|}\sum_{k \in \mathcal{P}_i} g(x_i; W^{\langle k \rangle}) \end{aligned} \tag{3}$$

Based on the formulation above, we propose SUGAR, a distributed training framework that: (1) partitions the input graph subject to resource constraints; (2) adopts local subgraph-level training. Figure 1 provides a simple illustration of SUGAR for a two-device system. We describe our design choices in detail in the following sections.

B. Theoretical Basis

Recall that we define a graph partitioning strategy $\mathcal{P}$ that divides N nodes into K node sets $(\mathcal{V}_1, \mathcal{V}_2, \cdots, \mathcal{V}_K)$. Taking K subgraphs induced by the node sets into consideration, a graph partitioning strategy $\mathcal{P}$ can be viewed as a way to produce a sparser adjacency matrix A_{SG}, from the original matrix A. A_{SG} is a block-diagonal matrix of A, *i.e.*,

$$A_{SG} = \begin{bmatrix} A_{\mathcal{V}_1} & \cdots & 0 & \cdots & 0 \\ \vdots & \ddots & & & \vdots \\ 0 & & A_{\mathcal{V}_k} & & 0 \\ \vdots & & & \ddots & \vdots \\ 0 & \cdots & 0 & \cdots & A_{\mathcal{V}_K} \end{bmatrix} \tag{4}$$

where $A_{\mathcal{V}_k}$ denotes the adjacency matrix of subgraph k.

We show below that adopting A_{SG} for training offers the benefits of high computational efficiency and low memory requirements. Moreover, we provide the error bound and convergence analysis of this approximation for a graph convolutional network (GCN) [14].

Complexity Analysis. The propagation rule for the l-th layer GCN is:

$$Z^{(l+1)} = A^{norm} H^{(l)} W^{(l)}, H^{(l+1)} = \sigma(Z^{(l+1)}) \tag{5}$$

where σ represents an activation function, A^{norm} denotes the normalized version of A, *i.e.*, $A^{norm} = \hat{D}^{-1/2}\hat{A}\hat{D}^{1/2}$, $\hat{A} = A + I_N$, $\hat{D}_{ii} = \sum_j \hat{A}_{ij}$ and I_N is an N-dimensional identity matrix. $H^{(l)}$ and $H^{(l+1)}$ denotes the input and output feature matrices in layer l, respectively. $Z^{(l)}$ is the node feature matrix before the activation function in layer l and $Z^{(L)}$ denotes final node predictions (*i.e.*, output of the GCN). $W^{(l)} \in R^{F_l \times F_{l+1}}$ represents the weight matrix of layer l, where F_l and F_{l+1} is the input and output feature dimension, respectively. Therefore, for the l-th layer GCN, the *training time complexity* is $\mathcal{O}(|\mathcal{E}|F_l + NF_lF_{l+1})$ and *memory complexity* is $\mathcal{O}(NF_{l+1} + F_lF_{l+1})$. We make two observations here: (a) Real-world graphs are usually sparse and $\frac{|\mathcal{E}|}{N}$ is generally smaller than feature number F_{l+1}. Thus, the second term dominates the time complexity; (b) For large-scale graphs, the number of nodes N is much greater than the number of features. Consequently, $\mathcal{O}(NF_{l+1})$ dominates the memory complexity. It is easy to verify that the number of nodes N imposes a computation hurdle on training. Partitioning the input graph into K subgraphs reduces the number of nodes N to $N_k = |\mathcal{V}_k|$ for every local model. Since N_k is about $1/K$ of N, the proposed approach is expected to achieve up to K times speedup, and as little as $1/K$ of the original memory requirements.

Error Bound Analysis. Let our proposed estimator be SG. The l-th layer propagation rule of a GCN with the SG estimator is:

$$Z_{SG}^{(l+1)} = A_{SG}^{norm} H_{SG}^{(l)} W^{(l)}, H_{SG}^{(l+1)} = \sigma(Z_{SG}^{(l+1)}) \tag{6}$$

where $Z_{SG}^{(l+1)}$ and $H_{SG}^{(l+1)}$ denote the node representations produced by the SG estimator in layer $l+1$ before and after activation, respectively.

Assume that we run graph partitioning for M times to obtain a sample average of A_{SG}^{norm} before training. Let $\epsilon = \|A_{SG}^{norm} - A^{norm}\|_\infty$ denote the error in approximating A^{norm} with A_{SG}^{norm}. For simplicity, we will omit the superscript $norm$ from now on.

The following lemma states that the error of node predictions given by the SG estimator is bounded.

Lemma 1. *For a multi-layer GCN with fixed weights, assume that: (1) $\sigma(\cdot)$ is ρ-Lipschitz and $\sigma(0) = 0$, (2) input matrices A, X and model weights $\{W^{(l)}\}_{l=1}^{L}$ are all bounded, then there exists C such that $\left\|Z_{SG}^{(l)} - Z^{(l)}\right\|_\infty \leq C\epsilon, \forall l \in [L]$ and $\left\|H_{SG}^{(l)} - H^{(l)}\right\|_\infty \leq C\epsilon, \forall l \in [L-1]$.*

The proof of Lemma 1 is provided in Appendix I. Lemma 1 motivates us to design a graph partitioning method that generates small ϵ so that the output of the SG estimator is close to the exact value. This will be discussed in detail in the next subsection.

Convergence Analysis. Let W_t denote the model parameters at training epoch t and W_* denote the optimal model weights. $\nabla\mathcal{L}(W) = \frac{1}{N}\sum_{i=1}^{N} \frac{\partial f(y_i, z_i^{(L)})}{\partial W}$ and $\nabla\mathcal{L}_{SG}(W) = \frac{1}{N}\sum_{i=1}^{N} \frac{\partial f(y_i, z_{SG,i}^{(L)})}{\partial W}$ represent the gradients of the exact GCN and SG estimator with respect to model weights W, respectively.

Theorem 1 states that with high probability gradient descent training with the approximated gradients of the SG estimator (*i.e.*, $\nabla\mathcal{L}_{SG}(W)$) converges to a local minimum.

Theorem 1. *Assume that: (1) the loss function $\mathcal{L}(W)$ is ρ-smooth, (2) the gradients of the loss $\nabla\mathcal{L}(W)$ and $\nabla\mathcal{L}_{SG}(W)$ are bounded for any choice of W, (3) the gradient of the*

objective function $\frac{\partial f(y,z)}{\partial z}$ *is* ρ*-Lipschitz and bounded, (4) the activation function* $\sigma(\cdot)$ *is* ρ*-Lipschitz,* $\sigma(0) = 0$ *and its gradient is bounded,*

then there exists $C > 0$*, s.t.,* $\forall M, T$*, for a sufficiently small* δ*, if we run graph partitioning for* M *times and run gradient descent for* $R \leq T$ *epochs (where* R *is chosen uniformly from* $[T]$*, the model update rule is* $W_{t+1} = W_t - \gamma \nabla \mathcal{L}_{SG}(W_t)$*, and step size* $\gamma = \frac{1}{\rho\sqrt{T}}$*), we have:*

$$P(\mathbb{E}_R \|\nabla \mathcal{L}(W_R)\|_F^2 \leq \delta) \geq$$
$$1 - 2\exp\{-2M(\frac{\delta}{2C} - \frac{2\rho[\mathcal{L}(W_1) - \mathcal{L}(W_*)] + C - \delta}{2C(\sqrt{T}-1)})^2\}$$

With M and T increasing, the right-hand-side of the inequality becomes larger. This implies that there is a higher probability for the loss to converge to a local minimum. The full proof is provided in Appendix I.

C. Graph Partitioning

From Lemma 1, we conclude that a graph partitioning method that yields a smaller $|A_{SG} - A|$ leads to a smaller error in node predictions. Therefore, we aim at minimizing the difference between A_{SG} and A. In other words, the objective of graph partitioning should be to *minimize the number of edges of the incident nodes* that belong to different subsets. As such, this is identical to the goal of various existing graph partitioning methods, making such approaches good candidates to use with our framework. We choose METIS [13] due to its efficiency in handling large-scale graphs. However, the traditional graph partitioning algorithms are *not* intended for modern GNNs and the learning component of the problem is missing. Consequently, we present a modified version of METIS that is suited to our problem and relies on two new ideas discussed next.

a) Weighted Graph Construction. We build a weighted graph $\mathcal{G}^w$ from the input graph $\mathcal{G}$. The *weight* of an edge e_{uv} is defined based on the degree of its two incident nodes:

$$\begin{aligned} weight(e_{uv}) &= d_{max} + 1 - deg(u) - deg(v) \\ d_{max} &= max\{deg(u) + deg(v), \forall e_{uv} \in \mathcal{E}\} \end{aligned} \tag{7}$$

Let A^w denote the adjacency matrix of the weighted graph $\mathcal{G}^w$, where element a_{ij}^w is the edge weight $weight(e_{ij})$; a_{ij}^w is 0 if there is no edge connecting nodes i and j.

The key intuition behind our first idea lies in the neighborhood aggregation scheme of GNNs. Consider two nodes u and v, where u is a hub node connected to many other nodes, while v has only one neighbor. As GNNs propagate by aggregating the neighborhood information of nodes, removing the only edge of node v may possibly lead to wrong predictions. On the other hand, pruning an edge of u is more acceptable since there are many neighbors contributing to its prediction. Consider the graph in Figure 1 as an example. Cutting the edges $e_1 \cup e_2$ and $e_3 \cup e_4$ are both feasible solutions for METIS. However, considering the fact that nodes connected to e_1 and e_2 have less topology information, our proposed method will preserve them and cut edges $e_3 \cup e_4$ instead; this can lead to a better learning performance.

As can be concluded from this small example, edges connected to small-degree nodes are critical to our problem and should be preserved. Conversely, edges connected to high-degree nodes may be intentionally ignored. This explains our weights definition strategy. Consequently, we incorporate the above observation into our partitioning objective and apply METIS to the pre-processed graph $\mathcal{G}^w$.

b) Subgraph Expansion. After obtaining the partitions with our modified METIS, we propose the second idea, *i.e.*, expand the subgraph based on available hardware resources. Although METIS only provides partitioning results where the node sets do not overlap, our general formulation in Section III-A allows nodes to belong to multiple partitions. This brings great flexibility to our approach to adjust the node number for each device according to its memory budget.

Suppose the available memory of device k is larger than the actual requirement of training a GNN on subgraph k (*i.e.*, $H(\mathcal{SG}_k) < B_{MEM}^k$), then we may choose to expand the node set $\mathcal{V}_k$ by adding the one-hop neighbors of nodes that do not belong to $\mathcal{V}_k$. As illustrated in Figure 1 (a), we can expand the node set of the subgraph on device 0 (marked in light brown) to include node n_0 as well. While expanding the subgraph is likely to yield higher accuracy, training time and memory requirement will also increase. Therefore, this is an optional step, only if the hardware resources allow it.

D. Subgraph-level Local Training

From the original formulation in Equation 3, if $|\mathcal{P}_i| > 1$, *i.e.*, a node i is assigned to multiple devices, calculating its loss and backpropagation can involve heavy communication among devices. To address this problem, we provide the following result to decouple the training of K local GNN models from each other.

Proposition 1. *If* $f(y, z)$ *is convex with respect to* z*, then the upper bound of* $\mathcal{L}$ *in Equation 3 is given by:*

$$\begin{aligned} \mathcal{L} &\leq \frac{1}{K}\sum_{k=1}^{K}\sum_{i\in\mathcal{V}_k}\frac{1}{|\mathcal{P}_i|}f(y_i, z_i) \\ z_i &= g(x_i, W^{\langle k\rangle}) \end{aligned} \tag{8}$$

The proof is provided in Appendix II.

Proposition 1 allows us to shift the perspective from 'node-level' to 'device-level'. We adopt the upper bound of $\mathcal{L}$ in Equation 8 as the new training objective. Now, the local model updates involving node i *do not* depend on other models (*i.e.*, $\{W^{\langle k\rangle}\}_{k\in\mathcal{P}_i}$) any more. Optimizing the new objective naturally reduces the upper bound of the original one and avoids significant communication costs, thus leading to high training efficiency.

Furthermore, motivated by deployment challenges in real IoT applications, where communication among devices is generally not guaranteed, we propose to reduce inter-device communication down to zero in our framework. In particular,

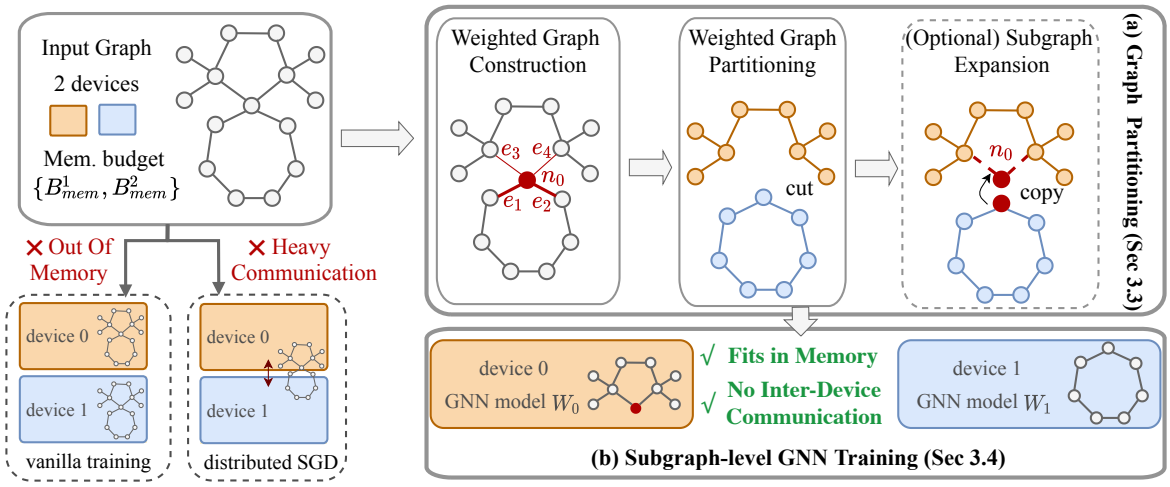


Fig. 1. While vanilla training is likely to run out of memory when the graph size is large and distributed stochastic gradient descent (SGD) requires heavy intermediate communication among devices, SUGAR provides a solution that is memory efficient and requires no inter-device communication. The proposed SUGAR consists of two stages: (a) graph partitioning and (b) subgraph-level GNN training. Graph partitioning involves three steps: (1) transform the input graph $\mathcal{G}$ to a weighted graph $\mathcal{G}^w$; (2) apply METIS to the weighted graph $\mathcal{G}^w$, where edges with large weights are more likely to be preserved; (3) (optional) expand the node set of the obtained subgraph according to memory budgets.

we maintain K distinct (local) models instead of a single (global) model by keeping the local model updates within each device. The objective of our proposed subgraph-level local GNN training can be summarized as follows:

$$\min_{W^{\langle k \rangle}} \mathcal{L}_k = \sum_{i \in \mathcal{V}_k} \frac{1}{|\mathcal{P}_i|} f(y_i, z_i), \ \forall k \in [K] \\ z_i = g(x_i, W^{\langle k \rangle}) \tag{9}$$

In training round t, every device performs local updates as:

$$W^{\langle k \rangle}_{t+1} \leftarrow W^{\langle k \rangle}_t - \gamma \nabla_{W^{\langle k \rangle}} \mathcal{L}_k, \ \forall k \in [K] \tag{10}$$

where $\mathcal{L}_k$ denotes the training objective of device k and γ is the learning rate (*i.e.*, step size). By decoupling training dependency among devices, we propose a feasible solution to train GNNs in resource-limited scenarios, where typical distributed GNN approaches are not applicable.

E. Putting it all together

Algorithm 1 SUGAR

Input: graph $\mathcal{G} = (\mathcal{V}, \mathcal{E})$; node feature matrix X; available device number K; device memory budget $\{B^k_{MEM}\}^K_{k=1}$; total training epochs T.

1: Construct $\mathcal{G}^w$ from $\mathcal{G}$ according to Equation 7
2: Partition $\mathcal{G}^w$ into K subgraphs $\{\mathcal{SG}_i\}^K_1$
3: (Optional) Expand $\mathcal{SG}_i$ if $H(\mathcal{SG}_i) < B^i_{MEM}$
4: **for** each device $k = \{1, 2, \cdots, K\}$ in parallel **do**
5: Initialize GNN model weight $W^{\langle k \rangle}_1$
6: **for** epoch $t = 1, 2, \cdots, T$ **do**
7: $W^{\langle k \rangle}_{t+1} \leftarrow W^{\langle k \rangle}_t - \gamma \nabla_{W^{\langle k \rangle}} \mathcal{L}_k$
8: **end for**
9: **end for**

To sum up, the SUGAR algorithm consists of two stages: (a) graph partitioning (lines 1-3) and (b) subgraph-level GNN training (lines 4-9). Specifically, the graph partitioning involves three steps: (1) construct a weighted graph $\mathcal{G}^w$ from $\mathcal{G}$ to account for the influence of node degrees in learning (line 1). (2) Apply METIS to the weighted graph $\mathcal{G}^w$ to obtain partitioning results (line 2). (3) According to the memory budget, expand the subgraph to cover the one-hop neighbors for better performance (line 3). Then, we train K local models in parallel without requiring training-time communication among devices (lines 4-9). The proposed subgraph-level training with multiple devices achieves high training efficiency, low memory requirements and zero communication costs.

IV. Experiments

A. Experimental Setup

We perform a thorough evaluation of SUGAR on five node classification benchmarks, *i.e.*, *Flickr*, *Reddit*, *ogbn-arxiv*, *ogbn-proteins* and *ogbn-products* [11], [16]. Dataset statistics are summarized in Table I. More details of the datasets are in Appendix III.

We include the following GNN architectures and training algorithms for comparison: (1) GCN [14], (2) GraphSAGE [9]: mini-batch GraphSAGE are denoted by GraphSAGE-mb, (3) GAT [21], (4) SIGN [7], (5) ClusterGCN [5], (6) GraphSAINT [27]: the random node, random edge, and random walk based samplers are denoted by GraphSAINT-N, GraphSAINT-E, GraphSAINT-RW, respectively. Descriptions about these GNN baselines are in Appendix III.

SUGAR is implemented with PyTorch [19] and DGL [22]. For all the baseline methods, we use the parameters reported in their github pages or the original paper. We report accuracy results averaged over 5 runs for *ogbn-proteins* and 10 runs for the other datasets.

TABLE I
DATASET STATISTICS. K AND M DENOTE 1,000 AND 1,000,000, RESPECTIVELY. 'AVGDEG.' REPRESENTS THE AVERAGE NODE DEGREE. 'ACC' DENOTES ACCURACY.

Dataset	*Flickr*	*Reddit*	*ogbn-arxiv*	*ogbn-proteins*	*ogbn-products*
#Nodes	89.3K	233K	169K	133K	2,449K
#Edges	0.90M	11.6M	1.17M	39.6M	61.9M
AvgDeg.	10	50	13.77	597	50.5
#Tasks	1	1	1	112	1
#Classes	7	41	40	2	47
Metric	ACC	ACC	ACC	ROC-AUC	ACC

For completeness, we run our experiments across multiple hardware platforms. We select five different devices with various computing and memory capabilities, namely, (1) Raspberry Pi 3B, (2) NVIDIA Jetson Nano, (3) Android phone with Snapdragon 845 processor, (4) laptop with Intel i5-8279U CPU, and (5) desktop with AMD Threadripper 3970X CPU and two NVIDIA RTX 3090 GPUs.

B. Results

1) Evaluations on GPUs: First, we provide evaluation of SUGAR on a two-GPU system. Table II and Table III report the average training time per epoch, maximum GPU memory usage and accuracy on *ogbn-arxiv* and *Reddit*. We base SUGAR on full-batch GCN and GraphSAGE for these two datasets, respectively. As shown in these tables, when compared with full-batch methods (*i.e.*, GCN and GAT for *ogbn-arxiv*; GraphSAGE for *Reddit*), SUGAR is much more memory efficient, as it reduces the peak memory by $1.7\times$ for *ogbn-arxiv* and $3.8\times$ for *Reddit* data. When compared against mini-batch methods (*i.e.*, mini-batch GraphSAGE, ClusterGCN, GraphSAINT and SIGN), the runtime of SUGAR is significantly smaller. This demonstrates the great benefits of our proposed subgraph-level training. Indeed, by restricting the neighborhood search size, SUGAR effectively alleviates the neighborhood expansion problem. In addition, it achieves very competitive test accuracies.

TABLE II
RUNTIME, MEMORY & ACCURACY RESULTS ON *ogbn-arxiv*. 'AVG. TIME' IS THE TRAINING TIME PER EPOCH AVERAGED OVER 100 EPOCHS AND 'MAX MEM' DENOTES PEAK ALLOCATED MEMORY ON GPU.

	Avg. Time [ms]	SUGAR Speedup	Max Mem [GB]	Test Acc. [%]
GCN	26.9	1.68×	1.60	72.37 ± 0.10
GAT	207.8	12.99×	5.41	72.95 ± 0.14
GraphSAGE	534.7	33.42×	0.95	71.98 ± 0.17
SIGN	291.6	18.23×	0.94	71.79 ± 0.08
SUGAR	16.0		0.92	72.22 ± 0.14

We also combine SUGAR with popular mini-batch training methods. For the largest *ogbn-products* dataset, we implement SUGAR together with three competitive GNN baselines, namely GraphSAGE, ClusterGCN and GraphSAINT. The results are summarized in Table IV. SUGAR provides a better solution that leads to runtime speedup, memory reduction and even a slightly increased test accuracy for all three methods. We hypothesize that the graph partitioning eliminates some task-irrelevant edges in the original graph, and thus leads to better generalization of GNNs.

Table V provides results on the dense *ogbn-proteins* graph. When it comes to training GNNs on dense graphs, memory poses a significant challenge due to the neighborhood expansion problem. The results show that GAT suffers from considerable memory usage. In contrast, SUGAR effectively alleviates the issue with $1.52\times$ runtime speedup and $1.73\times$ memory reduction. Due to space limitations, our results on *Flickr* data are presented in Appendix IV.

TABLE III
RUNTIME, MEMORY & ACCURACY RESULTS ON *Reddit*.

	Avg. Time [ms]	SUGAR Speedup	Max Mem [GB]	Test Acc. [%]
GraphSAGE	110.6	1.87×	5.70	96.39 ± 0.03
GraphSAGE-mb	316.5	5.36×	2.33	95.08 ± 0.05
ClusterGCN	414.4	7.01×	1.83	96.34 ± 0.01
GraphSAINT-N	341.8	5.78×	1.29	96.17 ± 0.06
GraphSAINT-E	299.8	5.07×	1.22	96.15 ± 0.06
GraphSAINT-RW	467.5	7.91×	1.23	96.23 ± 0.06
SIGN	352.8	5.97×	2.17	96.12 ± 0.05
SUGAR	59.1		1.51	96.01 ± 0.03

TABLE IV
RUNTIME, MEMORY & ACCURACY RESULTS ON *ogbn-products*.

	Avg. Time [ms]	Max Mem [GB]	Test Acc. [%]
GraphSAGE-mb	2.42	7.29	79.25 ± 0.22
SUGAR	1.49	4.43	79.97 ± 0.23
Improvement	1.62×	1.65×	0.72 (↑)
ClusterGCN	2.90	6.59	78.51 ± 0.33
SUGAR	1.97	3.36	79.34 ± 0.41
Improvement	1.47×	1.96×	0.83 (↑)
GraphSAINT-E	0.30	7.16	79.54 ± 0.27
SUGAR	0.28	3.92	80.20 ± 0.23
Improvement	1.07×	1.83×	0.66 (↑)

TABLE V
RUNTIME, MEMORY & ACCURACY RESULTS ON *ogbn-proteins*.

	Avg. Time [sec]	Max Mem [GB]	Valid Acc. [%]	Test Acc. [%]
GAT	6.20	10.77	92.08 ± 0.08	87.20 ± 0.17
SUGAR	4.09	6.22	92.51 ± 0.08	86.41 ± 0.18
Improvement	1.52×	1.73×	0.43 (↑)	0.79 (↓)

TABLE VI

AVERAGE TRAINING TIME PER EPOCH [SEC] OF SUGAR COMPARED WITH GRAPHSAINT AND GCN ON *Flickr* AND *ogbn-arxiv* DATA. WE RECORD THE TRAINING TIME ON FIVE PLATFORMS WITH CPU MODELS LISTED. OOM DENOTES OUT OF MEMORY. WE NOTE THAT TRAINING A GCN ON RASPBERRY PI 3B IS INFEASIBLE SINCE IT EXCEEDS MEMORY, WHILE SUGAR STILL WORKS.

Dataset		RPi 3B Cortex-A53	Jetson Cortex-A57	Phone SDM-845	Laptop i5-8279U	Desktop-CPU Zen2 3970X	Desktop-GPU RTX3090
Flickr	GraphSAINT-N	104.1	16.86	7.67	2.86	1.48	0.097
	SUGAR	48.2	7.61	3.54	1.21	0.67	0.050
	Speedup	2.16×	2.22×	2.17×	2.36×	2.24×	1.94×
ogbn-arxiv	GCN	OOM	28.10	21.96	13.80	5.16	0.027
	SUGAR	501.59	18.39	13.33	6.51	2.71	0.016
	Speedup	-	1.53×	1.65×	2.12×	1.91×	1.69×

TABLE VII

RUNTIME COMPARISON AGAINST BASELINE METHODS ON THREE LARGE DATASETS. AVERAGE TRAINING TIME PER EPOCH [SEC] IS REPORTED. BASELINE REFERS TO GRAPHSAGE FOR *Reddit* AND *ogbn-products*. GAT IS THE BASELINE FOR *ogbn-proteins*.

	Reddit	ogbn-products	ogbn-proteins
Baseline	2.02	170.75	269.70
SUGAR	0.88	77.05	142.7
Speedup	2.30×	2.22×	1.89×

2) Evaluations on mobile and edge devices: Following the GPU setting, we proceed to evaluate SUGAR on mobile and edge devices with CPUs.

Training Time. Table VI presents the average training time per epoch of SUGAR compared with baselines on the *Flickr* and *ogbn-arxiv* datasets. Due to the relative small size of these two datasets, we are able to train GNNs on all five hardware devices, ranging from a Raspberry Pi 3B, to a desktop equipped with high-performance CPUs. We also list the runtime on GPUs in the last column for easy comparison.

From Table VI, we can see that SUGAR demonstrates consistent speedup across all platforms, achieving over 2× and 1.5× speedup on the *Flickr* and *ogbn-arxiv* datasets, respectively. In addition, training a GCN on the Raspberry Pi 3B fails due to running out of memory, while SUGAR demonstrates good memory scalability and hence it can be used with such a device with a limited memory budget (*i.e.*, 1GB in this case). This also holds true for the *Reddit* dataset:

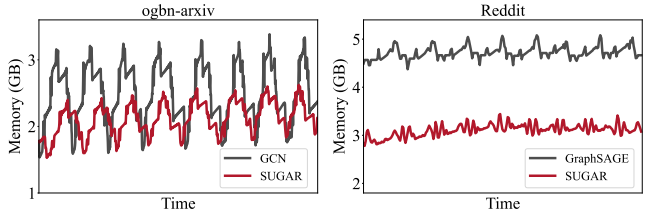


Fig. 2. Memory variation during training GNNs on Desktop-CPU for *ogbn-arxiv* and *Reddit*. For SUGAR, we plot the memory variation of the device that consumes most memory. More results are provided in Appendix IV.

SUGAR provides a feasible solution for local training on the Jetson Nano (time per epoch is 50.27s), while other baselines can not work due to large memory requirements.

Thus, for the other three datasets, we compare the runtime on Desktop-CPU and report our results in Table VII. We also observe consistent speedup across all datasets: SUGAR nearly halves the training time in all three cases.

Memory Usage. We compare the memory usage of SUGAR against GNN baselines on a CPU setting. Figure 2 illustrates the resident set size (RSS) memory usage during training on *ogbn-arxiv* and *Reddit*. Results on the other datasets are provided in Appendix IV. It is evident that our proposed SUGAR achieves substantial memory reductions. We emphasize that memory plays a critical role in GNN training. In the context of devices with limited resources, the situation is more severe since the graph dataset is already big and loading the full dataset may not be possible. By adopting subgraph-level training, SUGAR effectively alleviates the problem.

Finally, we present a case study of SUGAR on NVIDIA Jetson Nano in Appendix IV to demonstrate the applicability of SUGAR to edge devices.

C. Scalability Analysis

So far we have demonstrated the great performance of SUGAR with two available devices. A natural follow-up question is, *how does SUGAR perform on more devices, i.e., device number* $K > 2$. Due to space limitations, we provide a detailed scalability analysis in Appendix V. In short, we observe that there exists a tradeoff between training scalability and performance. With more number of devices available, SUGAR leads to greater training speedup and smaller memory usage at the cost of slightly degraded performance. Thus, this provides a feasible solution in extremely resource-limited scenarios while general GNN training methods are not applicable.

Finally, we study the influence of batch sizes on computational efficiency and memory scalability on SUGAR when compared with mini-batch training algorithms. Our results of a detailed analysis are provided in Appendix V.

V. CONCLUSION

We have proposed SUGAR, an efficient GNN training method that improves training scalability with multiple devices.

SUGAR can reduce computation, memory and communication costs during training through two key contributions: (1) a novel graph partitioning strategy with memory budgets and graph topology taken into consideration; (2) subgraph-level local GNN training. We have provided a theoretical analysis and conducted extensive experiments to demonstrate the efficiency of SUGAR with real datasets and hardware devices.

ACKNOWLEDGEMENTS

We thank Zhengqi Gao (*EECS Dept., MIT*) and Xinyuan Cao (*CS Dept., Gatech*) for their contributions in the theoretical derivations of this work. In particular, Zhengqi Gao proposed key proofs for Theorem 2 and Proposition 1 in the paper. The authors want to give gratitude to them for their invaluable help and support.

REFERENCES

[1] Hessam Bagherinezhad, Mohammad Rastegari, and Ali Farhadi. Lcnn: Lookup-based convolutional neural network. In *IEEE Conference on Computer Vision and Pattern Recognition*, July 2017.

[2] Jianfei Chen, Jun Zhu, and Le Song. Stochastic training of graph convolutional networks with variance reduction, 2018.

[3] Jie Chen, Tengfei Ma, and Cao Xiao. Fastgcn: Fast learning with graph convolutional networks via importance sampling, 2018.

[4] Tianlong Chen, Yongduo Sui, Xuxi Chen, Aston Zhang, and Zhangyang Wang. A unified lottery ticket hypothesis for graph neural networks. In *International Conference on Machine Learning*, pages 1695–1706. PMLR, 2021.

[5] Wei-Lin Chiang, Xuanqing Liu, Si Si, Yang Li, Samy Bengio, and Cho-Jui Hsieh. Cluster-gcn: An efficient algorithm for training deep and large graph convolutional networks. In *International Conference on Knowledge Discovery & Data Mining*, pages 257–266, 2019.

[6] Wenqi Fan, Yao Ma, Qing Li, Yuan He, Eric Zhao, Jiliang Tang, and Dawei Yin. Graph neural networks for social recommendation. In *The World Wide Web Conference*, pages 417–426, 2019.

[7] Fabrizio Frasca, Emanuele Rossi, Davide Eynard, Ben Chamberlain, Michael Bronstein, and Federico Monti. Sign: Scalable inception graph neural networks, 2020.

[8] Peter W Glynn and Dirk Ormoneit. Hoeffding's inequality for uniformly ergodic markov chains. *Statistics & probability letters*, 56(2):143–146, 2002.

[9] William L. Hamilton, Rex Ying, and Jure Leskovec. Inductive representation learning on large graphs. In *Proceedings of the 31st International Conference on Neural Information Processing Systems*, page 1025–1035, 2017.

[10] Kaiming He, Xiangyu Zhang, Shaoqing Ren, and Jian Sun. Deep residual learning for image recognition. In *IEEE Conference on Computer Vision and Pattern Recognition (CVPR)*, pages 770–778, 2016.

[11] Weihua Hu, Matthias Fey, Marinka Zitnik, Yuxiao Dong, Hongyu Ren, Bowen Liu, Michele Catasta, and Jure Leskovec. Open graph benchmark: Datasets for machine learning on graphs, 2021.

[12] Peter Kairouz, H Brendan McMahan, Brendan Avent, Aurélien Bellet, Mehdi Bennis, Arjun Nitin Bhagoji, Kallista Bonawitz, Zachary Charles, Graham Cormode, Rachel Cummings, et al. Advances and open problems in federated learning. *arXiv preprint arXiv:1912.04977*, 2019.

[13] George Karypis and Vipin Kumar. A fast and high quality multilevel scheme for partitioning irregular graphs. *SIAM Journal on scientific Computing*, 20(1):359–392, 1998.

[14] Thomas N. Kipf and Max Welling. Semi-supervised classification with graph convolutional networks. In *International Conference on Learning Representations*, 2017.

[15] Marek Kuczma. *An introduction to the theory of functional equations and inequalities: Cauchy's equation and Jensen's inequality*. Springer Science & Business Media, 2009.

[16] Jure Leskovec and Andrej Krevl. SNAP Datasets: Stanford large network dataset collection. http://snap.stanford.edu/data, June 2014.

[17] Jiayu Li, Tianyun Zhang, Hao Tian, Shengmin Jin, Makan Fardad, and Reza Zafarani. Sgcn: A graph sparsifier based on graph convolutional networks. In *Pacific-Asia Conference on Knowledge Discovery and Data Mining*, pages 275–287. Springer, 2020.

[18] Dongsheng Luo, Wei Cheng, Wenchao Yu, Bo Zong, Jingchao Ni, Haifeng Chen, and Xiang Zhang. Learning to drop: Robust graph neural network via topological denoising. In *International Conference on Web Search and Data Mining*, pages 779–787, 2021.

[19] Adam Paszke, Sam Gross, Francisco Massa, Adam Lerer, James Bradbury, Gregory Chanan, Trevor Killeen, Zeming Lin, Natalia Gimelshein, Luca Antiga, et al. Pytorch: An imperative style, high-performance deep learning library. *Advances in Neural Information Processing Systems*, 32:8026–8037, 2019.

[20] Yu Rong, Wenbing Huang, Tingyang Xu, and Junzhou Huang. Dropedge: Towards deep graph convolutional networks on node classification. In *International Conference on Learning Representations*, 2020.

[21] Petar Veličković, Guillem Cucurull, Arantxa Casanova, Adriana Romero, Pietro Liò, and Yoshua Bengio. Graph attention networks, 2018.

[22] Minjie Wang, Da Zheng, Zihao Ye, Quan Gan, Mufei Li, Xiang Song, Jinjing Zhou, Chao Ma, Lingfan Yu, Yu Gai, Tianjun Xiao, Tong He, George Karypis, Jinyang Li, and Zheng Zhang. Deep graph library: A graph-centric, highly-performant package for graph neural networks, 2020.

[23] Cameron R. Wolfe, Jingkang Yang, Arindam Chowdhury, Chen Dun, Artun Bayer, Santiago Segarra, and Anastasios Kyrillidis. Gist: Distributed training for large-scale graph convolutional networks, 2021.

[24] Chuhan Wu, Fangzhao Wu, Yang Cao, Yongfeng Huang, and Xing Xie. Fedgnn: Federated graph neural network for privacy-preserving recommendation, 2021.

[25] Felix Wu, Amauri Souza, Tianyi Zhang, Christopher Fifty, Tao Yu, and Kilian Weinberger. Simplifying graph convolutional networks. In *International conference on machine learning*, pages 6861–6871. PMLR, 2019.

[26] Zonghan Wu, Shirui Pan, Fengwen Chen, Guodong Long, Chengqi Zhang, and S Yu Philip. A comprehensive survey on graph neural networks. *IEEE Transactions on Neural Networks and Learning Systems*, 32(1):4–24, 2020.

[27] Hanqing Zeng, Hongkuan Zhou, Ajitesh Srivastava, Rajgopal Kannan, and Viktor Prasanna. Graphsaint: Graph sampling based inductive learning method. In *International Conference on Learning Representations*, 2020.

[28] Muhan Zhang and Yixin Chen. Link prediction based on graph neural networks. *Advances in Neural Information Processing Systems*, 31:5165–5175, 2018.

[29] Lingxiao Zhao and Leman Akoglu. Pairnorm: Tackling oversmoothing in gnns, 2020.

[30] Da Zheng, Chao Ma, Minjie Wang, Jinjing Zhou, Qidong Su, Xiang Song, Quan Gan, Zheng Zhang, and George Karypis. Distdgl: distributed graph neural network training for billion-scale graphs. In *Workshop on Irregular Applications: Architectures and Algorithms (IA3)*, pages 36–44. IEEE, 2020.

I. Theoretical Analysis (Section III, Page 3-4 in the paper)

In this section, we provide details of the following theoretical results used in the main paper:

(1) **Lemma 1**: For a multi-layer GCN with fixed weights, the error of the activations of the SG estimator are bounded.

(2) **Lemma 2**: For a multi-layer GCN with fixed weights, the error of the gradients of the SG estimator are bounded.

(3) **Theorem 1**: With high probability gradient descent training with the approximated gradients by the SG estimator can converge to a local minimum.

The proof builds on [2], but with different assumptions. More precisely, while [2] assume that model weights change slowly during training, our theoretical analysis is based on the difference in the adjacency matrices produced by graph partitioning.

A. Notations

Let $[L] = \{1, ..., L\}$. The infinity norm of a matrix is defined as $\|A\|_\infty = \max_{i,j} |A_{i,j}|$. By Proposition B in [2], we know that:

1) $\|AB\|_\infty \leq col(A)\|A\|_\infty \|B\|_\infty$
2) $\|A \circ B\|_\infty \leq \|A\|_\infty \|B\|_\infty$
3) $\|A + B\|_\infty \leq \|A\|_\infty + \|B\|_\infty$

where $col(A)$ represents the number of columns of matrix A and $\circ$ is the element-wise product. We define η to be the maximum number of columns we can possibly encounter in the proof.

We review some notations defined in the main text.[1] Our proposed estimator is denoted by SG. The propagation rule of a l-th layer GCN with the exact estimator is given by:

$$Z^{(l+1)} = A^{norm} H^{(l)} W^{(l)}, H^{(l+1)} = \sigma(Z^{(l+1)}) \tag{11}$$

Similarly, the propagation rule of a l-th layer GCN with the SG estimator is given by:

$$Z_{SG}^{(l+1)} = A_{SG}^{norm} H_{SG}^{(l)} W^{(l)}, H_{SG}^{(l+1)} = \sigma(Z_{SG}^{(l+1)}) \tag{12}$$

where σ represents an activation function, A^{norm} denotes the normalized version of A, *i.e.*, $A^{norm} = \hat{D}^{-1/2}\hat{A}\hat{D}^{1/2}, \hat{A} = A + I_N, \hat{D}_{ii} = \sum_j \hat{A}_{ij}$ and I_N is an N-dimensional identity matrix.$H^{(l)}$ and $H_{SG}^{(l)}$ denote node representations in the l-th layer produced by the exact GCN and SG estimator, respectively. $W^{(l)}$ represents the weight matrix in layer l. Note that while we write Equation 12 in a compact matrix form, in real implementation, the training process is distributed across K devices.

Recall that A_{SG} is a block-diagonal matrix produced by the graph partitioning module that serves as an approximation of A. Before training, we run graph partitioning for M times to obtain a sample average, *i.e.*, $A_{SG}^{norm} = \frac{1}{M}\sum_{m=1}^{M} A_{SG,m}^{norm}$. Let $\epsilon = \|A_{SG}^{norm} - A^{norm}\|_\infty$ denote the error in approximating A^{norm} with A_{SG}^{norm}. For simplicity, we will omit the superscript $norm$ from now on.

The model parameters at training epoch t are denoted by W_t. For W at a given time point (*i.e.*, fixed model weights), we omit the subscript in the proof. Let W_* denote the optimal model weights. $\nabla\mathcal{L}(W) = \frac{1}{N}\sum_{i=1}^{N} \frac{\partial f(y_i, z_i^{(L)})}{\partial W}$ and $\nabla\mathcal{L}_{SG}(W) = \frac{1}{N}\sum_{i=1}^{N} \frac{\partial f(y_i, z_{SG,i}^{(L)})}{\partial W}$ represent the gradients of the exact GCN and SG estimator with respect to model weights W, respectively. $f(\cdot, \cdot)$ is the objective function (*e.g.*, cross entropy for node classification tasks).

B. Activations of Multi-layer GCN

1) Single-layer GCN: Proposition 2 states that for a single-layer GCN, (1) the outputs are bounded if the inputs are bounded, (2) if the difference between the input of the SG estimator and the exact GCN is small, then the output of the SG estimator is close to the output of the exact GCN.

Proposition 2. *For a one-layer GCN, if the activation function $\sigma(\cdot)$ is ρ-Lipschitz and $\sigma(0) = 0$, for any input matrices A, A_{SG}, X, X_{SG} and any weight matrix W that satisfy:*

1) All the matrices are bounded by β: $\|A\|_\infty \leq \beta$, $\|A_{SG}\|_\infty \leq \beta$, $\|X\|_\infty \leq \beta$, $\|X_{SG}\|_\infty \leq \beta$ and $\|W\|_\infty \leq \beta$,

2) The differences between inputs are bounded: $\|X_{SG} - X\|_\infty \leq \alpha\epsilon$, where $\epsilon = \|A_{SG} - A\|_\infty$.

Then, there exist B and C that depend on ρ, η and β, s.t.,

1) The outputs are bounded: $\|H\|_\infty \leq B$ and $\|H_{SG}\|_\infty \leq B$,

2) The differences between outputs of the SG estimator and the exact estimator are bounded: $\|Z_{SG} - Z\|_\infty \leq C(1+\alpha)\epsilon$ and $\|H_{SG} - H\|_\infty \leq C(1+\alpha)\epsilon$.

Proof. We know that $\|Z\|_\infty = \|AXW\|_\infty \leq \eta^2\|A\|_\infty\|X\|_\infty\|W\|_\infty \leq \eta^2\beta^3$. By Lipschitz continuity of $\sigma(\cdot)$, $\|\sigma(Z) - \sigma(0)\|_\infty \leq \rho\eta^2\beta^3$ and we have $\|\sigma(Z)\|_\infty \leq \rho\eta^2\beta^3$. Thus $\|H\|_\infty \leq D$, where $B = \max\{\eta^2\beta^3, \rho\eta^2\beta^3\}$. Similarly, $\|H_{SG}\|_\infty \leq B$.

[1] Some equations in the Appendix may have different numbers from the main paper.

We proceed to show that the differences between outputs are bounded below:

$$\begin{aligned}\|Z_{SG} - Z\|_\infty &= \|A_{SG}X_{SG}W - AXW\|_\infty \\ &\leq \eta\|W\|_\infty\|A_{SG}X_{SG} - AX\|_\infty \\ &\leq \eta\beta(\|A_{SG}(X_{SG} - X)\|_\infty + \|X(A_{SG} - A)\|_\infty) \\ &\leq \eta\beta(\eta\beta\alpha\epsilon + \eta\beta\epsilon) \\ &= (1+\alpha)\eta^2\beta^2\epsilon\end{aligned} \tag{13}$$

By Lipschitz continuity of $\sigma(\cdot)$, we have $\|H_{SG} - H_t\|_\infty \leq \rho(1+\alpha)\eta^2\beta^2\epsilon$. Choose $C = \max\{(1+\alpha)\eta^2\beta^2, \rho(1+\alpha)\eta^2\beta^2\}$, and the proof is complete.

2) Multi-layer GCN: The following lemma relates the approximation error in activations (*i.e.*, $\left\|H_{SG}^{(l)} - H^{(l)}\right\|_\infty$) with the approximation error in input adjacency matrices (*i.e.*, $\epsilon = \|A_{SG} - A\|_\infty$).

Lemma 1. *For a multi-layer GCN with fixed model weights, given a (fixed) graph dataset, assume that:*

1) $\sigma(\cdot)$ is ρ-Lipschitz and $\sigma(0) = 0$,
2) The inputs are bounded by β: $\|A\|_\infty \leq \beta$, $\|A_{SG}\|_\infty \leq \beta$, $\|X\|_\infty \leq \beta$,
3) The model weights in each layer are bounded by β: $\left\|W^{(l)}\right\|_\infty \leq \beta, \forall l \in [L]$.

Then, there exist B and C that depend on ρ, η and β, s.t.,

1) $\left\|H^{(l)}\right\|_\infty \leq B, \left\|H_{SG}^{(l)}\right\|_\infty \leq B,\ \forall l \in [L-1]$,
2) $\left\|Z_{SG}^{(l)} - Z^{(l)}\right\|_\infty \leq C\epsilon,\ \forall l \in [L]$ and $\left\|H_{SG}^{(l)} - H^{(l)}\right\|_\infty \leq C\epsilon,\ \forall l \in [L-1]$.

Proof. Applying Proposition 2 to each layer of the GCN proves that $H^{(l)}$ and $H_{SG}^{(l)}$ are bounded for each layer l.
For the first layer of GCN, by Proposition 2 and input conditions, we know that there exists $C^{(1)}$ that satisfies:

$$\left\|Z_{SG}^{(1)} - Z^{(1)}\right\|_\infty \leq C^{(1)}\epsilon, \quad \left\|H_{SG}^{(1)} - H^{(1)}\right\|_\infty \leq C^{(1)}\epsilon$$

Note that for the first layer, the node feature matrix of the SG estimator and exact GCN are identical, *i.e.*, $X_{SG} = X$; this yields $\alpha = 0$ in Equation 13. Let $\hat{C}^{(1)} = C^{(1)}$. Next, we apply Proposition 2 to the second layer of GCN; there exists $C^{(2)}$ that satisfies:

$$\left\|Z_{SG}^{(2)} - Z^{(2)}\right\|_\infty \leq C^{(2)}(1+\hat{C}^{(1)})\epsilon, \quad \left\|H_{SG}^{(2)} - H^{(2)}\right\|_\infty \leq C^{(2)}(1+\hat{C}^{(1)})\epsilon$$

Let $\hat{C}^{(2)} = C^{(2)}(1+\hat{C}^{(1)})$. By applying Proposition 2 to the subsequent layer of GCN repetitively, we have $\hat{C}^{(l+1)} = C^{(l+1)}(1+\hat{C}^{(l)}), \forall l \in [L-1]$. We choose $C = \max_l \hat{C}^{(l)}$ and complete the proof.

C. Gradients of Multi-layer GCN

Lemma 2 below provides a bound for the difference between gradients of the loss by the SG estimator and the exact GCN (*i.e.*, $\|\nabla\mathcal{L}_{SG}(W) - \nabla\mathcal{L}(W)\|_\infty$). Intuitively, the gradient difference is small if the approximation error in input adjacency matrices (*i.e.*, ϵ) is small.

Lemma 2. *For a multi-layer GCN with fixed model weights, given a (fixed) graph dataset, assume that:*

1) $\frac{\partial f(y,z)}{\partial z}$ is ρ-Lipschitz and $\left\|\frac{\partial f(y,z)}{\partial z}\right\|_\infty \leq \beta$,
2) $\sigma(\cdot)$ is ρ-Lipschitz, $\sigma(0) = 0$ and $\|\sigma'(\cdot)\|_\infty \leq \beta$,
3) $\|A\|_\infty \leq \beta$, $\|A_{SG}\|_\infty \leq \beta$, $\|X\|_\infty \leq \beta$, $\left\|W^{(l)}\right\|_\infty \leq \beta, \forall l \in [L]$.

Then, there exists C that depends on ρ, η and β, s.t., $\|\nabla\mathcal{L}_{SG}(W) - \nabla\mathcal{L}(W)\|_\infty \leq C\epsilon$.

Proof. We begin by proving the following statements:
If the above assumptions hold, then there exist C and D that depends on ρ, η and β, s.t.,

1) The gradients with respect to the activations of each layer of the SG estimator are close to be unbiased:

$$\left\|\frac{\partial f}{\partial Z_{SG}^{(l)}} - \frac{\partial f}{\partial Z^{(l)}}\right\|_\infty \leq C\epsilon, \quad \forall l \in [L] \tag{14}$$

2) The gradients above are bounded:

$$\left\|\frac{\partial f}{\partial Z_{SG}^{(l)}}\right\|_\infty \leq D\beta, \quad \left\|\frac{\partial f}{\partial Z^{(l)}}\right\|_\infty \leq D\beta, \quad \forall l \in [L] \tag{15}$$

We prove these statements by induction. First we show that Equations 14 and 15 hold true for the final layer of GCN (*i.e.*, $l = L$). By Assumption 1 and Lemma 1, we know that there exists $\hat{C}$ that satisfies:

$$\left\| \frac{\partial f}{\partial Z_{SG}^{(L)}} - \frac{\partial f}{\partial Z^{(L)}} \right\|_\infty \leq \rho \left\| Z_{SG}^{(L)} - Z^{(L)} \right\|_\infty \leq \rho \hat{C} \epsilon \tag{16}$$

Let $C^{(L)} = \rho \hat{C}$ and $D^{(L)} = 1$. Next, suppose the statements hold for layer $l+1$, *i.e.*, there exist $C^{(l+1)}$ and $D^{(l+1)}$ that satisfy:

$$\left\| \frac{\partial f}{\partial Z_{SG}^{(l+1)}} - \frac{\partial f}{\partial Z^{(l+1)}} \right\|_\infty \leq C^{(l+1)} \epsilon, \quad \left\| \frac{\partial f}{\partial Z_{SG}^{(l+1)}} \right\|_\infty \leq D^{(l+1)} \beta, \quad \left\| \frac{\partial f}{\partial Z^{(l+1)}} \right\|_\infty \leq D^{(l+1)} \beta \tag{17}$$

We derive the gradients of the objective function with respect to activations in layer l by chain rule:

$$\begin{aligned} \left\| \frac{\partial f}{\partial Z^{(l)}} \right\|_\infty &= \left\| \sigma'(Z^{(l)}) \circ \frac{\partial f}{\partial H^{(l)}} \right\|_\infty \\ &= \left\| \sigma'(Z^{(l)}) \circ A^T \ \frac{\partial f}{\partial Z^{(l+1)}} \ {W^{(l)}}^T \right\|_\infty \\ &\leq \eta^2 \left\| \sigma'(Z^{(l)}) \right\|_\infty \|A\|_\infty \left\| \frac{\partial f}{\partial Z^{(l+1)}} \right\|_\infty \left\| W^{(l)} \right\|_\infty \\ &\leq \eta^2 \beta^4 D^{(l+1)} \end{aligned} \tag{18}$$

Thus, we know that $\left\| \frac{\partial f}{\partial Z^{(l)}} \right\|_\infty \leq D^{(l)} \beta$. Similarly, $\left\| \frac{\partial f}{\partial Z_{SG}^{(l)}} \right\|_\infty \leq D^{(l)} \beta$, where $D^{(l)} = \eta^2 \beta^3 D^{(l+1)}$.

We proceed to derive the error of the gradients by the SG estimator in layer l:

$$\begin{aligned} \left\| \frac{\partial f}{\partial Z_{SG}^{(l)}} - \frac{\partial f}{\partial Z^{(l)}} \right\|_\infty &= \left\| \sigma'(Z_{SG}^{(l)}) \circ A_{SG}^T \ \frac{\partial f}{\partial Z_{SG}^{(l+1)}} \ {W^{(l)}}^T - \sigma'(Z^{(l)}) \circ A^T \ \frac{\partial f}{\partial Z^{(l+1)}} \ {W^{(l)}}^T \right\|_\infty \\ &\leq \eta \left\| W^{(l)} \right\|_\infty \left\| \sigma'(Z_{SG}^{(l)}) \circ A_{SG}^T \ \frac{\partial f}{\partial Z_{SG}^{(l+1)}} - \sigma'(Z^{(l)}) \circ A^T \ \frac{\partial f}{\partial Z^{(l+1)}} \right\|_\infty \\ &\leq \underbrace{\eta\beta \left\| (\sigma'(Z_{SG}^{(l)}) - \sigma'(Z^{(l)})) \circ A_{SG}^T \frac{\partial f}{\partial Z_{SG}^{(l+1)}} \right\|_\infty}_{(*)} + \underbrace{\eta\beta \left\| \sigma'(Z^{(l)}) \circ A_{SG}^T (\frac{\partial f}{\partial Z_{SG}^{(l+1)}} - \frac{\partial f}{\partial Z^{(l+1)}}) \right\|_\infty}_{(**)} \\ &+ \underbrace{\eta\beta \left\| \sigma'(Z^{(l)}) \circ (A_{SG}^T - A^T) \frac{\partial f}{\partial Z^{(l+1)}} \right\|_\infty}_{(***)} \end{aligned} \tag{19}$$

By Assumption 2 and Lemma 1, we know that there exists $\hat{C}$ such that $\left\| \sigma'(Z_{SG}^{(l)}) - \sigma'(Z^{(l)}) \right\|_\infty \leq \rho \hat{C} \epsilon$. From Equation 17, we have:

$$\begin{aligned} \text{(*) in Equation (19)} &\leq \eta^2 \beta \left\| \sigma'(Z_{SG}^{(l)}) - \sigma'(Z^{(l)}) \right\|_\infty \|A_{SG}\|_\infty \left\| \frac{\partial f}{\partial Z_{SG}^{(l+1)}} \right\|_\infty \\ &\leq \eta^2 \beta \cdot \rho \hat{C} \epsilon \cdot \beta \cdot D^{(l+1)} \beta \\ &= (\eta^2 \beta^3 \rho \hat{C} D^{(l+1)}) \epsilon \\ \text{(**) in Equation (19)} &\leq \eta^2 \beta \left\| \sigma'(Z^{(l)}) \right\|_\infty \|A_{SG}\|_\infty \left\| \frac{\partial f}{\partial Z_{SG}^{(l+1)}} - \frac{\partial f}{\partial Z^{(l+1)}} \right\|_\infty \\ &\leq \eta^2 \beta \cdot \beta \cdot \beta \cdot C^{(l+1)} \epsilon \\ &= (\eta^2 \beta^3 C^{(l+1)}) \epsilon \\ \text{(***) in Equation (19)} &\leq \eta^2 \beta \left\| \sigma'(Z^{(l)}) \right\|_\infty \left\| A_{SG}^T - A^T \right\|_\infty \left\| \frac{\partial f}{\partial Z^{(l+1)}} \right\|_\infty \\ &\leq \eta^2 \beta \cdot \beta \cdot \epsilon \cdot D^{(l+1)} \beta \\ &= (\eta^2 \beta^3 D^{(l+1)}) \epsilon \end{aligned} \tag{20}$$

Therefore, $\left\|\frac{\partial f}{\partial Z_{SG}^{(l)}} - \frac{\partial f}{\partial Z^{(l)}}\right\|_\infty \leq C^{(l)}\epsilon$, where $C^{(l)} = \eta^2\beta^3[(\rho\hat{C}+1)D^{(l+1)} + C^{(l+1)}]$. By induction, Equations 14 and 15 hold true.

Next, we show below that there exists C that depends on ρ, η and β, *s.t.*,

$$\left\|\frac{\partial f}{\partial W_{SG}^{(l)}} - \frac{\partial f}{\partial W^{(l)}}\right\|_\infty \leq C\epsilon, \quad \forall l \in [L] \tag{21}$$

By backpropagation rule we derive that $\frac{\partial f}{\partial W^{(l)}} = (AH^{(l)})^T\frac{\partial f}{\partial Z^{(l)}}$. By Lemma 1, we know that $H_{SG}^{(l)}$ is bounded by some $\hat{B}$ and $\left\|H_{SG}^{(l)} - H^{(l)}\right\|_\infty \leq \tilde{C}\epsilon$ hold for some $\tilde{C}$. From the previous proof, we know that there exists $\hat{C}$ and $\hat{D}$, *s.t.*, Equations 14 and 15 hold; thus, we have:

$$\begin{aligned}
\left\|\frac{\partial f}{\partial W_{SG}^{(l)}} - \frac{\partial f}{\partial W^{(l)}}\right\|_\infty &\leq \left\|(A_{SG}H_{SG}^{(l)})^T\frac{\partial f}{\partial Z_{SG}^{(l+1)}} - (AH^{(l)})^T\frac{\partial f}{\partial Z^{(l+1)}}\right\|_\infty \\
&\leq \left\|(A_{SG}H_{SG}^{(l)})^T(\frac{\partial f}{\partial Z_{SG}^{(l+1)}} - \frac{\partial f}{\partial Z^{(l+1)}})\right\|_\infty + \left\|((A_{SG}H_{SG}^{(l)})^T - (AH^{(l)})^T)\frac{\partial f}{\partial Z^{(l+1)}}\right\|_\infty \\
&\leq \eta^2\beta\cdot\hat{B}\cdot\hat{C}\epsilon + \eta\left\|A_{SG}H_{SG}^{(l)} - AH^{(l)}\right\|_\infty\hat{D}\beta \\
&\leq \eta^2\beta\hat{B}\hat{C}\epsilon + \eta\beta\hat{D}\left\|A_{SG}(H_{SG}^{(l)} - H^{(l)})\right\|_\infty + \eta\beta\hat{D}\left\|(A_{SG}-A)H^{(l)}\right\|_\infty \\
&\leq \eta^2\beta\hat{B}\hat{C}\epsilon + \eta\beta\hat{D}\cdot\eta\beta\cdot\tilde{C}\epsilon + \eta\beta\hat{D}\cdot\eta\epsilon\cdot\hat{B} \\
&= \eta^2\beta(\hat{B}\hat{C} + \beta\tilde{C}\hat{D} + \hat{B}\hat{D})\epsilon
\end{aligned} \tag{22}$$

Therefore, Equation 21 holds, where $C = \eta^2\beta(\hat{B}\hat{C} + \beta\tilde{C}\hat{D} + \hat{B}\hat{D})$.

Finally, we have: $\|\nabla\mathcal{L}_{SG}(W) - \nabla\mathcal{L}(W)\|_\infty \leq C\epsilon$, and the proof is complete.

D. Convergence Analysis

Theorem 1. *Assume that:*

1) *The loss function $\mathcal{L}(W)$ is ρ-smooth, i.e., $|\mathcal{L}(W_2) - \mathcal{L}(W_1) - \langle\mathcal{L}(W_1), W_2 - W_1\rangle| \leq \frac{\rho}{2}\|W_2 - W_1\|_F^2, \forall W_1, W_2$, where $\langle A, B\rangle = tr(A^TB)$ denotes the inner product of matrix A and B,*
2) *The gradients of the loss $\nabla\mathcal{L}(W)$ and $\nabla\mathcal{L}_{SG}(W)$ are bounded by G for any choice of W,*
3) *The gradient of the objective function $\frac{\partial f(y,z)}{\partial z}$ is ρ-Lipschitz and bounded,*
4) *The activation function $\sigma(\cdot)$ is ρ-Lipschitz, $\sigma(0) = 0$ and $\sigma'(\cdot)$ is bounded.*

Then there exists $C > 0$, s.t., $\forall M, T$, for a sufficiently small δ, if we run graph partitioning for M times and run gradient descent for $R \leq T$ epochs (where R is chosen uniformly from $[T]$, the model update rule is $W_{t+1} = W_t - \gamma\nabla\mathcal{L}_{SG}(W_t)$, step size $\gamma = \frac{1}{\rho\sqrt{T}}$), we have:

$$P(\mathbb{E}_R\|\nabla\mathcal{L}(W_R)\|_F^2 \leq \delta) \geq 1 - 2\exp\{-2M(\frac{\delta}{2C} - \frac{2\rho[\mathcal{L}(W_1) - \mathcal{L}(W_*)] + C - \delta}{2C(\sqrt{T}-1)})^2\}$$

Proof. Let $\delta_t = \nabla\mathcal{L}_{SG}(W_t) - \nabla\mathcal{L}(W_t)$ denote the differences between gradients at epoch t. By ρ-smoothness of $\mathcal{L}(W)$ we know that:

$$\begin{aligned}
\mathcal{L}(W_{t+1}) &\leq \mathcal{L}(W_t) + \langle\nabla\mathcal{L}(W_t), W_{t+1} - W_t\rangle + \frac{\rho}{2}\gamma^2\|\nabla\mathcal{L}_{SG}(W_t)\|_F^2 \\
&= \mathcal{L}(W_t) - \gamma\langle\nabla\mathcal{L}(W_t), \nabla\mathcal{L}_{SG}(W_t)\rangle + \frac{\rho}{2}\gamma^2\|\nabla\mathcal{L}_{SG}(W_t)\|_F^2 \\
&= \mathcal{L}(W_t) - \gamma\langle\nabla\mathcal{L}(W_t), \delta_t\rangle - \gamma\|\nabla\mathcal{L}(W_t)\|_F^2 + \frac{\rho}{2}\gamma^2[\|\delta_t\|_F^2 + \|\nabla\mathcal{L}(W_t)\|_F^2 + 2\langle\delta_t, \nabla\mathcal{L}(W_t)\rangle] \\
&= \mathcal{L}(W_t) - (\gamma - \rho\gamma^2)\langle\nabla\mathcal{L}(W_t), \delta_t\rangle - (\gamma - \frac{\rho}{2}\gamma^2)\|\nabla\mathcal{L}(W_t)\|_F^2 + \frac{\rho}{2}\gamma^2\|\delta_t\|_F^2
\end{aligned} \tag{23}$$

By Lemma 2, we know that at a given time point t, there exists $\hat{C}$ *s.t.*, δ_t is bounded by $\hat{C}\epsilon$. Therefore,

$$\begin{aligned}
&|\langle\nabla\mathcal{L}(W_t), \delta_t\rangle| \leq \eta\|\nabla\mathcal{L}(W_t)\|_\infty\|\delta_t\|_\infty \leq \eta G\hat{C}\epsilon \\
&\|\delta_t\|_F^2 \leq \|\nabla\mathcal{L}_{SG}(W_t)\|_\infty^2 + \|\nabla\mathcal{L}(W_t)\|_\infty^2 \leq 2G^2
\end{aligned} \tag{24}$$

Let $C = \max\{\eta G\hat{C}, 2G^2\}$. Equation 23 can be further derived as:

$$\mathcal{L}(W_{t+1}) \leq \mathcal{L}(W_t) + (\gamma - \rho\gamma^2)C\epsilon - (\gamma - \frac{\rho}{2}\gamma^2)\|\nabla\mathcal{L}(W_t)\|_F^2 + \frac{\rho}{2}C\gamma^2 \tag{25}$$

By summing up the above inequalities from $t = 1$ to T and rearranging the terms, we have:

$$(\gamma - \frac{\rho}{2}\gamma^2) \sum_t \|\nabla \mathcal{L}(W_t)\|_F^2 \leq \mathcal{L}(W_1) - \mathcal{L}(W_*) + CT(\gamma - \rho\gamma^2)\epsilon + \frac{\rho}{2}CT\gamma^2 \tag{26}$$

Dividing both sides of Equation 26 by $T(\gamma - \frac{\rho}{2}\gamma^2)$ and choosing $\gamma = \frac{1}{\rho\sqrt{T}}$ gives us:

$$\begin{aligned}
\mathbb{E}_R\|\nabla \mathcal{L}(W_R)\|_F^2 &\leq 2\frac{\mathcal{L}(W_1) - \mathcal{L}(W_*) + CT(\gamma - \rho\gamma^2)\epsilon + \frac{\rho}{2}CT\gamma^2}{T\gamma(2 - \rho\gamma)} \\
&\leq \frac{2[\mathcal{L}(W_1) - \mathcal{L}(W_*)]}{T\gamma} + 2C(1 - \rho\gamma)\epsilon + \rho C\gamma \\
&\leq \frac{2\rho[\mathcal{L}(W_1) - \mathcal{L}(W_*)]}{\sqrt{T}} + 2C(1 - \frac{1}{\sqrt{T}})\epsilon + \frac{C}{\sqrt{T}} \\
&\leq \frac{2\rho[\mathcal{L}(W_1) - \mathcal{L}(W_*)] + C}{\sqrt{T}} + 2C(1 - \frac{1}{\sqrt{T}})\epsilon
\end{aligned} \tag{27}$$

Recall that ϵ denotes the infinity norm of the error in approximating A through M runs, *i.e.*, $\epsilon = \|A_{SG} - A\|_\infty$. Applying Hoeffding's inequality [8] to the largest element of the matrix $|A_{SG} - A|$ (which are bounded by the intervals $[0, 1]$), we have:

$$P(\epsilon \geq \delta) \leq 2\exp(-2M\delta^2), \quad \forall \delta \geq 0 \tag{28}$$

Combining the two inequalities above, we have:

$$\begin{aligned}
P(\mathbb{E}_R\|\nabla \mathcal{L}(W_R)\|_F^2 \geq \delta) &\leq P(\frac{2\rho[\mathcal{L}(W_1) - \mathcal{L}(W_*)] + C}{\sqrt{T}} + 2C(1 - \frac{1}{\sqrt{T}})\epsilon \geq \delta) \\
&\leq 2\exp\{-2M(\frac{\delta}{2C} - \frac{2\rho[\mathcal{L}(W_1) - \mathcal{L}(W_*)] + C - \delta}{2C(\sqrt{T} - 1)})^2\}
\end{aligned} \tag{29}$$

Therefore, for a sufficiently small δ, we have the following inequality for $P(\mathbb{E}_R\|\nabla \mathcal{L}(W_R)\|_F^2 \leq \delta)$:

$$P(\mathbb{E}_R\|\nabla \mathcal{L}(W_R)\|_F^2 \leq \delta) \geq 1 - 2\exp\{-2M(\frac{\delta}{2C} - \frac{2\rho[\mathcal{L}(W_1) - \mathcal{L}(W_*)] + C - \delta}{2C(\sqrt{T} - 1)})^2\} \tag{30}$$

Theorem 1 is proved.

II. Proof of Proposition 1 (Section III, Page 4 in the paper)

By convexity of f, using Jensen's inequality [15] gives us:

$$f(y_i, \frac{1}{|\mathcal{P}_i|}\sum_{k \in \mathcal{P}_i} g(x_i; W^{\langle k \rangle}) \leq \frac{1}{|\mathcal{P}_i|}\sum_{k \in \mathcal{P}_i} f(y_i, g(x_i; W^{\langle k \rangle})) \tag{31}$$

By changing the operation order and regrouping the indices, we further derive:

$$\frac{1}{N}\sum_{i=1}^{N}\frac{1}{|\mathcal{P}_i|}\sum_{k \in \mathcal{P}_i} f(y_i, z_i) = \frac{1}{K}\sum_{k=1}^{K}\sum_{i \in \mathcal{V}_k}\frac{1}{|\mathcal{P}_i|} f(y_i, z_i) \tag{32}$$

Therefore,

$$\begin{aligned}
\mathcal{L} &\leq \frac{1}{K}\sum_{k=1}^{K}\sum_{i \in \mathcal{V}_k}\frac{1}{|\mathcal{P}_i|} f(y_i, z_i) \\
z_i &= g(x_i, W^{\langle k \rangle})
\end{aligned} \tag{33}$$

Proposition 1 is proved.

III. Experimental Setup (Section IV, Page 5 in the paper)

We evaluate SUGAR on five node classification datasets, selected from very diverse applications: (1) categorizing types of images based on the descriptions and common properties of online images (*Flickr*); (2) predicting communities of online posts based on user comments (*Reddit*); (3) predicting the subject areas of arxiv papers based on its title and abstract (*ogbn-arxiv*); (4) predicting the presence of protein functions based on biological associations between proteins (*ogbn-proteins*); (5) predicting the category of a product in an Amazon product co-purchasing network (*ogbn-products*). Note that the task of *ogbn-proteins* is multi-label classification, while other tasks are multi-class classification.

We include the following GNN architectures and SOTA GNN training algorithms for comparison:

- GCN [14]: Full-batch Graph Convolutional Networks.
- GraphSAGE [9]: An inductive representation learning framework that efficiently generates node embeddings for previously unseen data.
- GAT [21]: Graph Attention Networks, a GNN architecture that leverages masked self-attention layers.
- SIGN [7]: Scalable Inception Graph Neural Networks, an architecture using graph convolution filters of different size for efficient computation.
- ClusterGCN [5]: A mini-batch training technique that partitions the graphs into a fixed number of subgraphs and draws mini-batches from them.
- GraphSAINT [27]: A mini-batch training technique that constructs mini-batches by graph sampling.

Note that our reported experiments involve no training communication among local models, *i.e.*, K local models are trained separately. While training with communication (*e.g.*, maintain a central model to collect gradient updates from local models and do the gradient descent) aligns rigorously with our theoretical analysis in Section III-B and is expected to achieve higher accuracy than training without communication, the latter yields great practical benefits as (1) communication is not guaranteed in many real IoT applications, (2) savings in communication costs lead to training speedup, as well as energy reduction per device, which are crucial for model deployment in practice. Moreover, we observed that training without communication already yields satisfactory results compared with its counterpart. For instance, we conducted experiments on *ogbn-arxiv* graph with both settings, and the difference in test accuracy is small (*i.e.*, 0.08% for a two-device system and 0.47% for a eight-device system). Thus, we adopt the no training-time communication setting due to its practical value and empirically good performance.

IV. More Experimental Results (Section IV, Page 6-7 in the paper)

Table VIII presents results of SUGAR integrated with GraphSAINT for three sampler modes (*i.e.*, node, edge, and random walk based samplers) on *Flickr*. Note that the accuracy we obtain (about 50%) is consistent with results in [27]. SUGAR achieves more than 2× runtime speedup and requires less memory than GraphSAINT. Of note, the test accuracy loss is within 1% in all cases.

TABLE VIII
Runtime, memory & accuracy results on *Flickr*.

	Avg. Time [ms]	Max Mem [GB]	Test Acc. [%]
GraphSAINT-N	97.0	0.41	50.64 ± 0.28
SUGAR	49.9	0.31	50.11 ± 0.12
Improvement	1.94×	1.32×	0.53 (↓)
GraphSAINT-E	71.1	0.53	50.91 ± 0.12
SUGAR	32.6	0.41	49.96 ± 0.12
Improvement	2.18×	1.29×	0.95 (↓)
GraphSAINT-RW	108.9	0.65	51.03 ± 0.20
SUGAR	37.3	0.49	50.15 ± 0.24
Improvement	2.92×	1.33×	0.88 (↓)

Figure 3 compares the resident set size (RSS) memory usage of SUGAR against GNN baselines on a CPU setting on the four datasets: *Reddit*, *ogbn-arxiv*, *ogbn-proteins* and *ogbn-products*. We train a full-batch version of GCN and the batch size of GAT is larger compared with GraphSAGE and GraphSAINT. This accounts for higher fluctuation in the corresponding figure. It is evident that our proposed SUGAR achieves substantial memory reductions compared with baseline GNNs.

We present a case study of SUGAR on NVIDIA Jetson Nano in Table IX. Jetson Nano is a popular, cheap and readily available platform (we adopt the model with quad Cortex-A57 CPU and 4GB LPDDR memory) and thus considered as a good fit for our problem scenario. Apart from training time, we measure the peak RSS memory usage for the training process and calculate energy consumption. As shown in Table IX, SUGAR achieves low latency, consumes less memory and is more

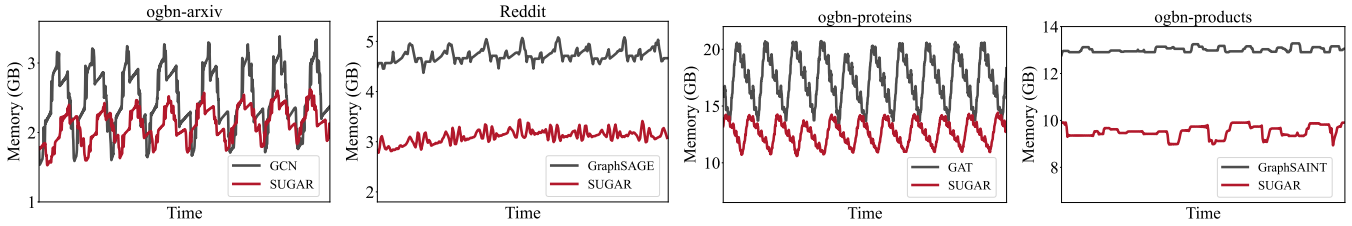


Fig. 3. Memory variation during training GNNs on Desktop-CPU for the four datasets: *ogbn-arxiv*, *Reddit*, *ogbn-proteins* and *ogbn-products*. For SUGAR, we plot the memory variation of the device that consumes most memory. As it can be seen, the memory requirements for SUGAR are significantly smaller than baseline methods.

energy efficient than baseline GNN algorithms. Therefore, it provides an ideal choice to train GNNs on devices with limited memory and battery capacity.

TABLE IX

EVALUATIONS OF SUGAR ON NVIDIA JETSON NANO FOR *Flickr* AND *ogbn-arxiv*. 'AVG. TIME' AND 'MAX MEM' DENOTES TRAINING TIME PER EPOCH AND PEAK RESIDENT SET SIZE (RSS) MEMORY. WE MEASURE THE TIME, MEMORY AND ENERGY FOR TRAINING 10 EPOCHS. SUGAR IMPROVES AVERAGE TRAINING TIME, MEMORY USAGE AND ENERGY CONSUMPTION PER DEVICE OVER BASELINE GNNS (*i.e.*, GRAPHSAINT AND GCN).

Dataset		Avg. Time [sec]	Max Mem [GB]	Energy [kJ]
Flickr	GraphSAINT-N	22.62	1.05	1.13
	SUGAR	10.50	0.89	0.52
	Improvement	2.15×	1.18×	2.17×
ogbn-arxiv	GCN	28.10	2.24	1.27
	SUGAR	18.39	1.46	0.81
	Improvement	1.53×	1.53×	1.57×

V. SCALABILITY ANALYSIS (SECTION IV, PAGE 7 IN THE PAPER)

A. Number of partitions

Below we provide a scalability analysis of SUGAR based on the number of partitions (*i.e.*, device number K).

We vary the number of available devices K from 2 to 8 and evaluate SUGAR on the *ogbn-arxiv*, *Reddit* and *ogbn-products* datasets. The evaluation is conducted on Desktop-GPU. Runtime speedup, peak GPU memory reduction, validation and test accuracy are presented in Figure 4. With increasing K, we observe a decreased training time and peak memory usage for each local device.

As we can see, while distributing the GNN model to more devices yields computation efficiency, test accuracy drops a bit. For instance, in the case of 8 devices, the biggest decrease happens in the *ogbn-products* dataset: test accuracy is 76.69% while the baseline accuracy is 79.54%. In the meantime, SUGAR leads to $5.13\times$ speedup, as well as $4.24\times$ memory reduction compared with the baseline. Generally speaking, there exists a tradeoff between training scalability and performance. The underlying reason is that the increase of partition number K leads to more inter-device edges, which corresponds to a larger error in estimating with A_{SG} with A.

We further evaluated SUGAR in a 128-device setting. The results show that the test accuracy drop compared with baseline GNNs is small, *i.e.*, within 5% when scaling up to 128 devices (*e.g.*, accuracy decreases from 72.37% to 67.80% for *ogbn-arxiv*, from 96.39% to 92.32% for *Reddit*, from 50.64% to 46.31% for *Flickr*). At the same time, we note that the memory savings are great (*e.g.*, peak memory usage per device is reduced from 1.60GB to 0.02GB for *ogbn-arxiv*). This shows that SUGAR can work with very small computation and memory requirements at the cost of slightly downgraded performance. Thus, this provides a feasible solution in extremely resource-limited scenarios while general GNN training methods are not applicable.

B. Batch Size

For mini-batch training algorithms, when the limited memory of device renders GNN training infeasible, a natural idea is reduce the batch size for memory savings. Here, we analyze the influence of SUGAR and the act of reducing batch sizes on computational efficiency, as well as memory scalability. We conduct experiments on the largest *ogbn-products* graph with GraphSAGE as the baseline. Two settings are considered: (a) graph data loaded on CPU, longer training time and smaller memory consumption is expected; (b) graph data loaded on GPU, the model runs faster, yet requires more GPU memory. Figure 5 in this Appendix provides runtime and memory results with varying batch sizes.

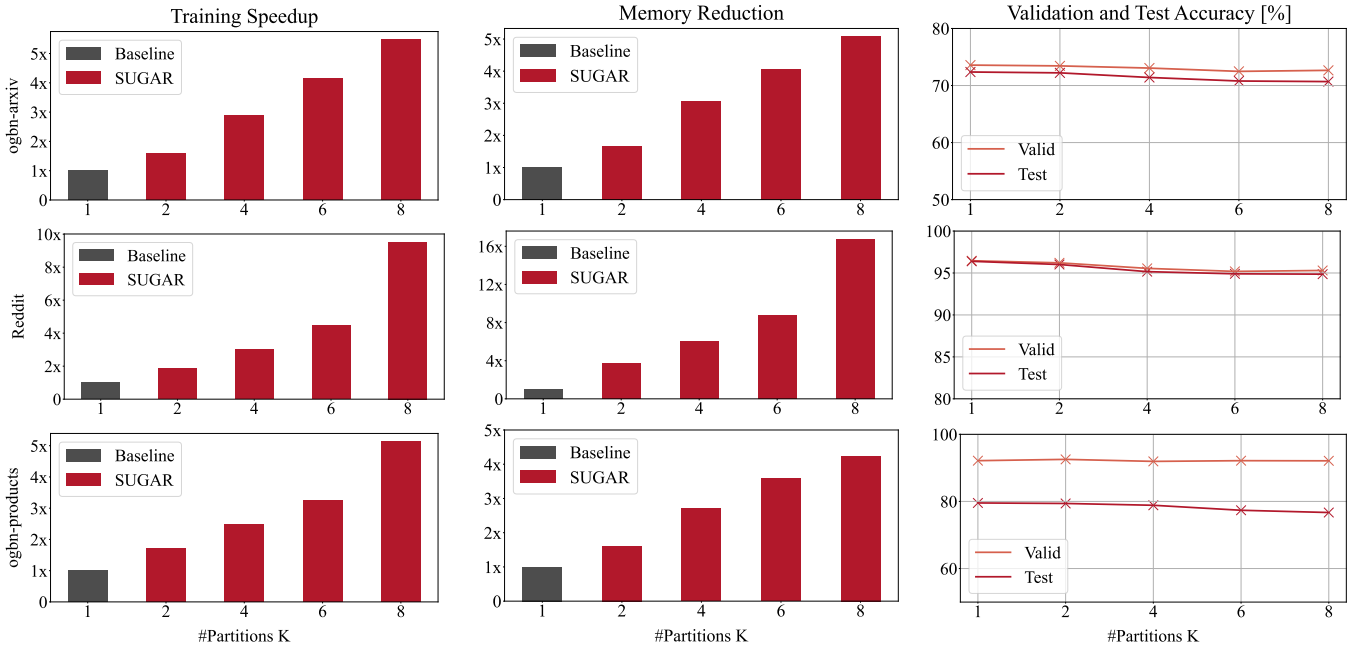
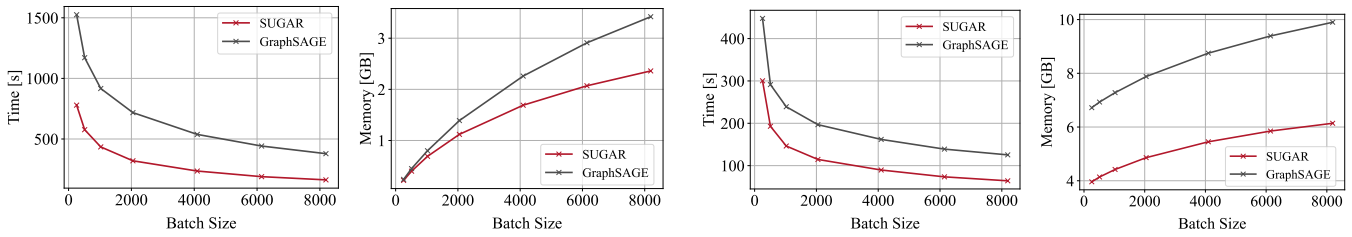


Fig. 4. Scalability analysis on the number of partitions (*i.e.*, the number of available devices K) for SUGAR. $K = 1$ refers to the baseline GNN (*i.e.*, GCN for *ogbn-arxiv*; GraphSAGE for *Reddit*; GraphSAINT for *ogbn-products*). We report the smallest training time speedup and peak GPU memory reduction among K devices (*i.e.*, the worst-case scenario) of SUGAR over the baseline.



(a) graph data on CPU

(b) graph data on GPU

Fig. 5. The training time and peak GPU memory with varying batch sizes of GraphSAGE and SUGAR for the *ogbn-products* data. We investigate two settings: (a) graph data loaded on GPU for faster execution (b) graph data loaded on CPU for memory savings.

We have two observations: (1) SUGAR mainly improves runtime in setting (a) and achieves greater memory reduction in setting (b). This is related to the mechanism of SUGAR: each local model adopts one subgraph for training instead of the original graph; thus, data loading time is reduced in setting (a) and putting a subgraph on GPU is more memory efficient in setting (b). (2) SUGAR demonstrates to be a better technique in reducing memory usage than tuning the batch size. While it is generally known that there exists a tradeoff between computation and memory requirements as reducing batch size increases training time, SUGAR is able to improve on both accounts.